Astrophys Space Sci (2006) 306:217–229
DOI 10.1007/s10509-006-9253-2

ORIGINAL ARTICLE

Photometric and H_α Observations of the Cataclysmic Star UX UMa

Diana Kjurkchieva · Dragomir Marchev · Tatiana Khruzina · Gojko Djurašević

Received: 2 December 2005 / Accepted: 19 September 2006

Abstract UBVRI photometry and spectroscopic observations around the H_α line of the cataclysmic star UX UMa are presented. The analysis of the 9-year photometry shows that the out-of-eclipse brightness of the system and the depth of the eclipse changes in different time scales while the width of the eclipse remains constant. The observed features of the light curves as well as the features of the two-peaked H_α profiles were attributed to an inhomogeneity of the accretion disk. "Spiral arm" model for a fitting of the light curves of UX UMa is proposed. It reproduces well the observational data. The obtained azimuthal extent of the spiral arms is of $\sim 90^\circ$ and their light contribution is about 17–30% of the total V flux of the disk. The obtained two dense structures at the outer disk covering partially the inner hot disk and the white dwarf at orbital phases ~ 0.7 and ~ 0.2 is in agreement with the predictions of the theoretical computations.

Keywords Stars: binaries close · Binaries: eclipsing · Binaries: cataclysmic variables · Stars: individual: UX UMa · Stars

D. Kjurkchieva · D. Marchev
Department of Physics, Shumen University, 115 Universitetska Str. 9700 Shumen, Bulgaria

T. Khruzina (✉)
Sternberg Astronomical Institute, Universitetski pr. 13, Moscow 119992, Russia
e-mail: kts@sai.msu.ru

G. Djurašević
Astronomical observatory, Volgina 7, 11160 Belgrade, Serbia and Montenegro

1 Introduction

The star UX UMa is discovered in 1933 by Beljavski. After several years Zverev and Kukarkin determine its light curve as an Algol-type with one eclipse minimum. Linnell (1949) found the flickering and the stillstand on the rising branch of the eclipse minimum. Johnson et al. (1954) discovered the "hump" lasting around half an orbital period. The attempts of Krzeminski and Walker (1963) to find a secondary eclipse in the IR range were not successful. Mandel (1965) found that the orbital period varies with a period 10600 days.

The first model of this binary is given by Walker and Herbig (1954). According to the present model UX UMa is eclipsing cataclysmic star consisting of a white dwarf with an accretion disk and a late MS star filling-in its Roche lobe.

UX UMa is a prototype of the nova-like stars that are nonmagnetic cataclysmic stars with bright and stable disk. According to Meyer and Meyer-Hofmeister (1983) the nova-like stars are in state of permanent eruption due to the high accretion rate.

Dmitrienko (1994) carried out simultaneous UBVRI observations of UX UMa in 1985–1991 and concluded that the accretion disk around the white dwarf is highly inhomogeneous.

Warner and Nather (1972) found 29-sec oscillations of the light of UX UMa confirmed later by HST observations (Knigge et al., 1998). They are attributed to emission of hot compact region on the white dwarf surface.

Naylor et al. (1996) did not find linear polarization of the emission of UX UMa.

The X-ray spectrum of UX UMa is very soft compared to X-spectra of other nova-like stars. There is not a visible eclipse in the X-ray curve (Wood et al., 1995).

The HST UV spectroscopy (Baptista et al., 1995) show deep eclipse with steep branches but without a hump. The

features of the two branches of the UV minimum were interpreted by eclipse of the white dwarf. The IUE observations show also a high speed wind from the star.

There are emission lines of HeII, CIII and Balmer lines as well as absorption lines of HeI, MgII and H in the spectra of UX UMa (Suleimanov et al., 2004). The profiles of the emission lines are double-peaked (typical shape for an accretion disk) but their components do not disappear consecutively during the eclipse minimum (Holm et al., 1982; Schlegel et al., 1983). Third emission component of the hydrogen lines as well as wide H absorption in the phase range of the hump were also found (Schlegel et al., 1983).

According to the standard models of UX UMa the dominant emission source of the system is the accretion disk (with circular or elliptical shape) whose eclipse causes the light minimum. The second emission source is a hot spot created at the place where the accretion stream from the secondary star falls on the disk (Smak, 1970). These models were widely used for interpretation of the hump, flickering and standstill of the UX UMa light curves during the last 30 years (Bruch, 2000).

The models with a hot spot on the disk edge allow to fit well both shape and depth of the eclipse but are not able to reproduce the irregular changes of the out-of-eclipse part of the light curves.

According to the recent three-dimensional gas-dynamical investigations (Bisikalo et al., 1997a,b, 1998, 2005; Makita et al., 2000) the stream and the accretion disk of the close binaries represent an unified formation. Their interaction is independent on the gas temperatures at the outer parts of the disk and shockless for arbitrary initial conditions. This means that the place of increased energetic output is outside the disk. It is assumed that this region, called "hot line", is a result of the interaction of the disk halo and inter-component envelope with the gas stream (Bisikalo et al., 1998; Makita et al., 2000). The "hot line" model allows to fit the whole light curves including their changeable out-of-eclipse parts (Khruzina, 2001; Khruzina et al., 2003a,b).

The last studies of cataclysmic variables (CVs) with a low mass ratio ($q = M_{wd}/M_{rd} \leq 7$) show that one or two equal extended spiral arms can be formed in the outer parts of their accretion disks. The first arm is near the region of interaction of the gas stream and the disk and the second arm is at the opposite region of the disk (Harlaftis and Marsh, 1996; Steeghs, 2001). The tidal shock waves initiated by the massive secondary are the probable reason for the spiral arm formation. Theoretical investigation of Bisikalo et al. (1998) and Makita et al. (2000) show that the observed spiral structures of the accretion disks are waves of density. The denser masses behind the arms of the spiral shock wave have higher temperature than the surrounding disk (Kuznetsov et al., 2001). The increased velocity of the gas flows of these structures (due to the increased energetic output) are apparent on the Doppler tomograms. The spiral structure of the disk may be established by photometric observations of eclipsing systems with significant vertical inhomogeneities causing covering of the internal regions of the disk.

So far the conditions for formation of such vertical inhomogeneities of the spiral arms is poorly studied. The last three-dimensional gas-dynamical computations (Bisicalo et al., 2006) show that the gas of the external disk regions gets a vertical acceleration as a result of the interaction between the stream and the disk halo. Both the vertical motion of the gas and its motion along the external disk edge causes a gradual increase of the thickness the disk halo.

The computations show that the maximum thickness of the external disk halo corresponds to orbital phase $\sim 0.6-0.7$ and the second smaller maximum – to phase ~ 0.2. Dips (light decreases) of the out-of-eclipse light curve should appear when the line-of-sight crosses these large-scale inhomogeneities due to the covering of the internal hot disk regions and the white dwarf (Khruzina, 2005).

We carried out 9 year observations of UX UMa in order to study its long-term and short-term variability. Their analysis and modeling could throw an additional light on the accretion processes in this system as well as on the configuration of its accretion disk.

2 Observations

We obtained light curves of UX UMa during 8 nights at the end of 1992 and the beginning of 1993, 6 nights in 1996, 1 night in 1997, 5 nights in 2000 and 2 nights in 2001 (Table 1). All observations were carried out by two-channel photometer mounted on the 60-cm telescope (Kreiner et al., 1993) of the Mt. Suhora Observatory. The telescope is equipped by an autoguider (Krzesinski and Wojcik, 1993). The stars GSC 3469516, BD+52 1720 and BD+52 1722 were used as comparison stars in different seasons and BD+52 1715 (HD 118215) as a check star. A calibration of the channels was made every night. The integration times were 10–15 sec in the different filters. In order to search for short-period variabilities observations with integration time 2 sec were made also in B and no filter.

The accuracy of our photometric data is: 0.01 mag in B, V and R band; 0.02 mag in U and I band; 0.02–0.03 mag for the runs with 2-sec integration time.

The data are phased according to the ephemeris of Kreiner et al. (2001):

$$HJD(\mathrm{Min}I) = 2427341,2243 + 0.196671273 * E \qquad (1)$$

and Figs. 1–10 presents some of the obtained light curves in the instrumental system.

Table 1 Journal of observations

Date	HJD	Run start UT	Duration	Type of observation	Integration time
20/21 Dec. 92	2448976.0	$00^h\ 56^m$	$4^h\ 06^m$	no filter	10^s
22/23 Dec. 92	2448979.0	$00^h\ 13^m$	$4^h\ 47^m$	no filter	10^s
23/24 Dec. 92	2448980.0	$23^h\ 50^m$	$4^h\ 58^m$	no filter	10^s
24/25 Dec. 92	2448981.0	$20^h\ 22^m$	$5^h\ 43^m$	no filter	10^s
25/26 Dec. 92	2448982.0	$20^h\ 32^m$	$5^h\ 22^m$	U,B,V	10^s
26/27 Dec. 92	2448983.0	$20^h\ 45^m$	$7^h\ 49^m$	B,V	10^s
28/29 Dec. 92	2448985.0	$22^h\ 48^m$	$7^h\ 27^m$	U,B,V	10^s
02/03 Jan. 93	2448990.0	$23^h\ 32^m$	$5^h\ 33^m$	B	2^s
07/08 Apr. 96	2450181.0	$01^h\ 26^m$	$1^h\ 41^m$	B,V,R,I	10^s
08/09 Apr. 96	2450182.0	$20^h\ 25^m$	$6^h\ 25^m$	B,V,R,I	10^s
09/10 Apr. 96	2450183.0	$16^h\ 10^m$	$1^h\ 26^m$	B,V,R,I	10^s
10/11 Apr. 96	2450184.0	$21^h\ 11^m$	$5^h\ 30^m$	B,V,R,I	10^s
18/19 Apr. 96	2450192.0	$20^h\ 00^m$	$6^h\ 10^m$	B,V,R,I	10^s
04/05 May. 96	2450208.0	$20^h\ 30^m$	$1^h\ 54^m$	B,V,R,I	10^s
12/13 Mar. 97	2450520.0	$20^h\ 55^m$	$5^h\ 30^m$	B,V,R,I	10^s
22/23 Apr. 00	2451657.0	$20^h\ 40^m$	$5^h\ 10^m$	B,V,R	10^s
23/24 Apr. 00	2451658.0	$20^h\ 20^m$	$4^h\ 45^m$	B,V,R	15^s
03/04 May. 00	2451668.0	$21^h\ 30^m$	$4^h\ 05^m$	B,V,R	10^s
05/06 May. 00	2451670.0	$19^h\ 55^m$	$4^h\ 25^m$	no filter	2^s
10/11 May. 00	2451675.0	$20^h\ 35^m$	$4^h\ 20^m$	no filter	2^s
25/26 May. 00	2451690.0	$20^h\ 55^m$	$3^h\ 10^m$	H_α	20^m
17/18 Nov. 01	2452231.0	$00^h\ 45^m$	$3^h\ 40^m$	B	2^s
26/27 Nov. 01	2452240.0	$23^h\ 05^m$	$5^h\ 20^m$	B	2^s
01/04 Apr. 02	2452366.0	$23^h\ 04^m$	$3^h\ 05^m$	H_α	25^m
02/03 Apr. 02	2452367.0	$00^h\ 20^m$	$2^h\ 20^m$	H_α	25^m
04/05 Jul. 02	2452460.0	$20^h\ 10^m$	$3^h\ 20^m$	H_α	25^m

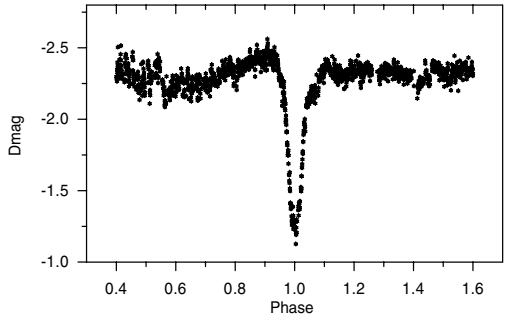

Fig. 1 B light curve of UX UMa from January 2, 1993 (integration time 2 sec)

UX UMa was observed also in the spectral range around the H_α line with resolution 0.19 Å/pixel in May 2000, April 2002 and June 2002 (Table 1). We used a CCD camera mounted on the Coude spectrograph (grating $B\&L632/14.7^\circ$) of the 2-m telescope of the National Astronomical Observatory at Rozhen (Bulgaria). The seeing during the observations did not exceed 2 arcsec (FWHM). The exposure time was 20–25 min and the ratio S/N was around 30. The bias frames and flat-field integrations were obtained at the beginning and end of each night. All stellar integrations were alternated with Th-Ar comparison source exposures. The data were processed in a standard way using

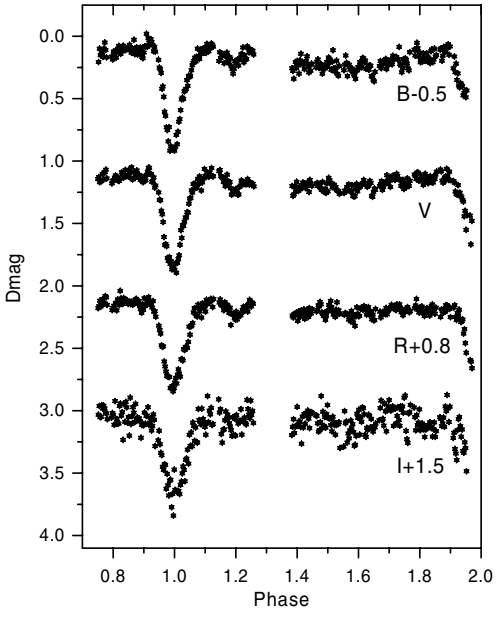

Fig. 2 BVRI light curves of UX UMa from April 8, 1996

the PCIPS (Smirnov, 1992) and Rewia (Borkowski, 1988) software packages. The spectra were reduced by bias substraction, flat-field division and wave-length calibration. The normalized spectra are shown in Figs. 11–14.

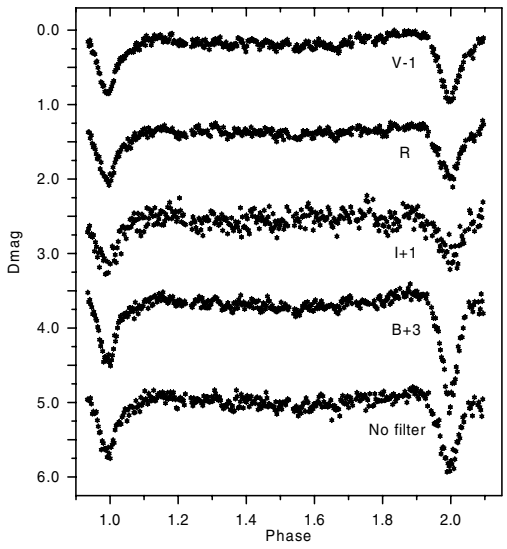

Fig. 3 BVRIN light curves of UX UMa from April 10, 1996

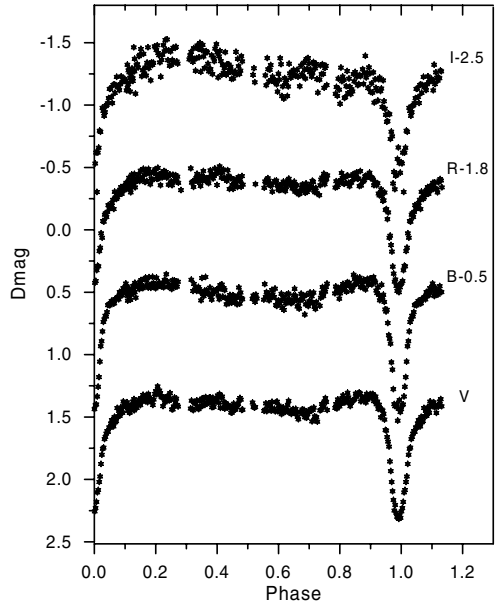

Fig. 4 BVRI light curves of UX UMa from March 12, 1997

3 Analysis of the photometric data

Our prolonged multicolor photometry (Figs. 1–10) reveals that the shape of the light curve of UX UMa is quite changeable.

(1) The out-of-eclipse brightness is minimum at the phase range 0.5–0.7 and maximum around the phase 0.9. The only exception is the light curve from April 23 2000 (Fig. 6) when the brightness is maximum at phase 0.1.
(2) Some photometric curves show light decreasing around phases 0.2–0.25 lasting nearly 1/10 of the orbital period. This feature is more apparent at the longer wavelengths.

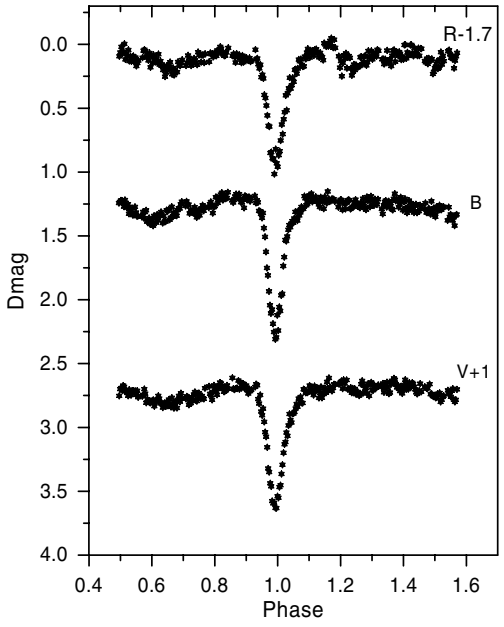

Fig. 5 BVR light curves of UX UMa from April 22, 2000

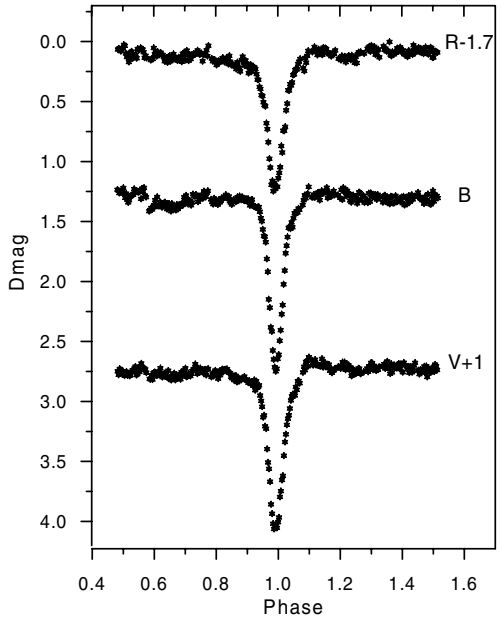

Fig. 6 BVR light curves of UX UMa from April 23, 2000

(3) The hump in the phase range 0.7–1.3 is well visible on almost all light curves. Its amplitudes are around 0.2 mag in B, 0.015 mag in V and 0.01 mag in R color. The hump is almost invisible in I color. There is not a hump on the light curve from April 23, 2000 which shape differs from all the rest also by the smaller brightness before the eclipse than after it. Both, the light curve obtained one day (April 22, 2000) before this "irregular" curve and the light curve obtained 10 days later (May 3, 2000) have a normal shape. Our results for the humps on the light curves of UX UMa confirm the conclusion of

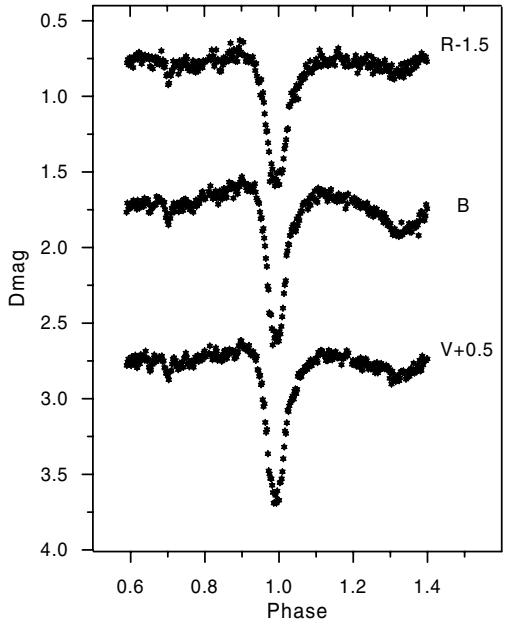

Fig. 7 BVR light curves of UX UMa from May 3, 2000

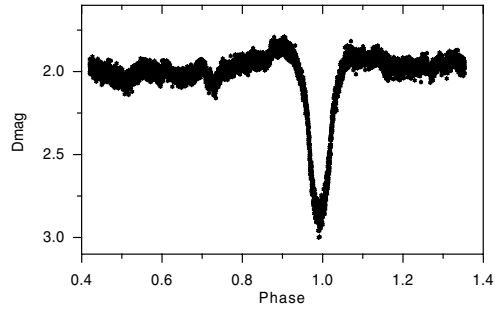

Fig. 8 No-filter light curve of UX UMa from May 5, 2000 (integration time 2 sec)

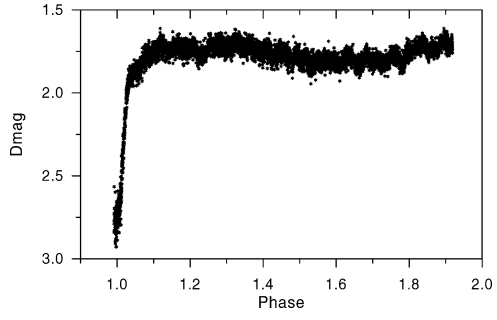

Fig. 9 No-filter light curves of UX UMa from May 10, 2000 (integration time 2 sec)

Dmitrienko (1994) about the variability of this feature (until the complete disappearance).

(4) The most light curves show a standstill on the increasing branch of the eclipse with different duration and shape. Sometimes the standstill is almost flat (especially in B color). There is a similar feature on the decreasing branch of the eclipse of the light curve from April 18, 1996. The light curve from May 5, 2000 shows a symmetric eclipse without standstill. These facts mean that if the hot spot is responsible for the standstill on the light curve then its location and luminosity changes during the different seasons.

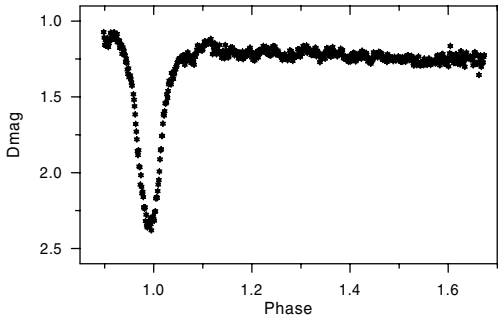

Fig. 10 B light curves of UX UMa from November 17, 2001 (integration time 2 sec)

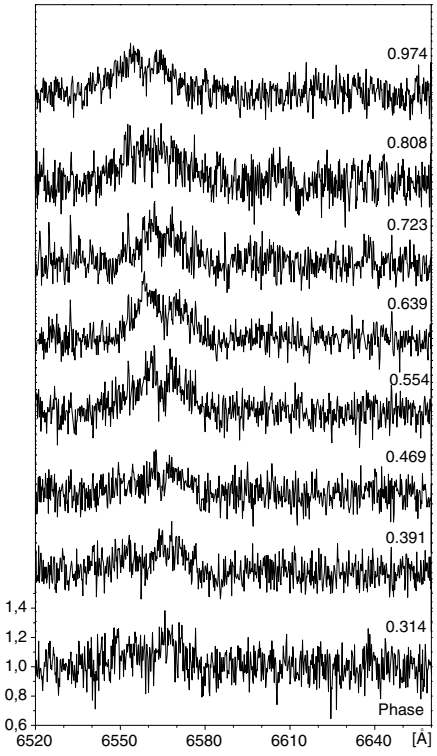

Fig. 11 H_α profiles of UX UMa from May 25, 2000

(5) The most of the light curve reveal brightness depression at phases 0.7 noted earlier by Dmitrienko (1994).

(6) The brightness of UX UMa increases or decreases simultaneously in all spectral bands. This conclusion is in correspondence of the result of Dmitrienko (1994).

(7) We assume that the phase 0.6 is the most appropriate phase for definition of the out-of-eclipse brightness. Our photometric data reveal that it changes in the different seasons by 1 mag in B, 0.9 mag in V, 1.56 mag in R and 0.86 mag in I color (Table 2). Dmitrienko (1994)

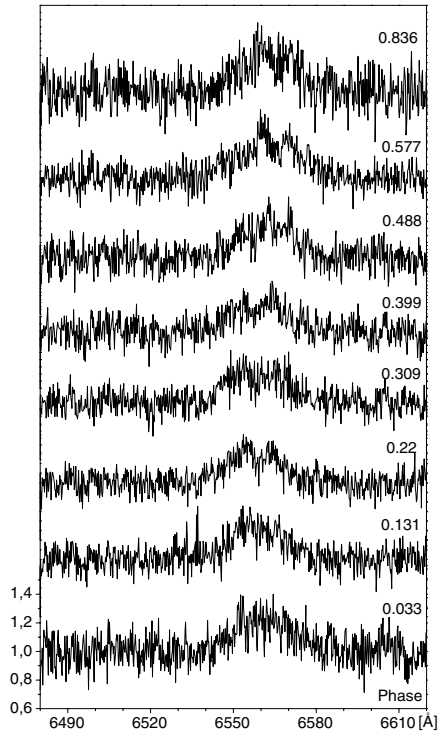

Fig. 12 H_α profiles of UX UMa from April 1, 2002

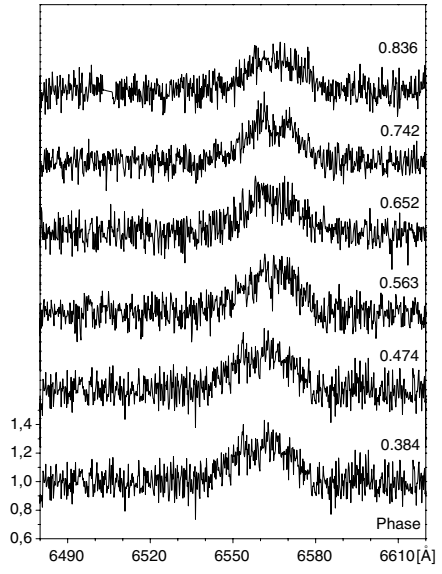

Fig. 13 H_α profiles of UX UMa from April 3, 2002

defined the out-of-eclipse brightness as a mean value for the phase range 0.2–0.5 and found amplitudes of the out-of-eclipse brightness variations 0.63 mag in U; 0.5 mag in B; 0.43 mag in V and 0.5 mag in R and I filter.

(8) The depths of the eclipse of our light curves change in the ranges (Table 2): 0.7–1.1 mag in B; 0.65–0.9 mag in V; 0.6–0.85 mag in R; 0.6–0.8 mag in I band. Only the light curve from April 23, 2000 is with an enormously big depth of the eclipse. Dmitrienko (1994) also has obtained two light curves with such a big eclipse depths.

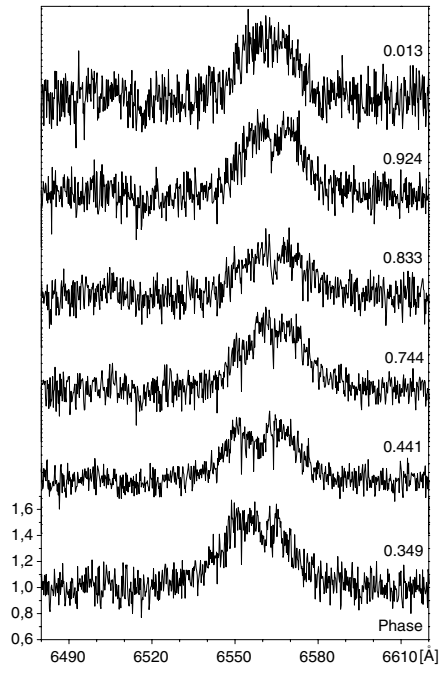

Fig. 14 H_α profiles of UX UMa from June 4, 2002

Our conclusion about the variability of the eclipse depth and the out-of-eclipse brightness variations of UX UMa coincides with those for the novalike systems RW Tri (Dmitrienko, 1991) and AC Cnc (Dmitrienko, 1992).

(9) We noted a trend of an increasing of the eclipse depth with the increasing of out-eclipse brightness (Table 2) that is more apparent at the shorter wavelengths.

(10) The data in Table 2 allow us to assume that the nova-like star UX UMa has different states similarly to the other types of CVs. Its states formally might be called low, intermediate and high. The out-of-eclipse brightness at low state is around 12.4 mag in B, 12 mag in V, 12.2 mag in R and 13.9 mag in I color with depths of the eclipse correspondingly 0.8 mag in both B and V color, 0.7 mag in both R and I color. The out-of-eclipse brightness at high state is around 11.5 mag in B, 11.7 mag in V and 11.4 mag in R color with depths of the eclipse above correspondingly 1.05 mag in B, 0.90 mag in V and 0.7 mag in R color. The light curves of the intermediate state (from March 12, 1997 and May 3, 2000) have almost the same out-of-eclipse brightness as that at low state while their eclipse depths are between those of high and low state. The light differences between the states of UX UMa are considerably smaller than those of the other types CVs (SS Cyg-type, AM Her-type, etc.) and the transitions between these states are rather continuous than abrupt.

Table 2 Long-term variability of UX UMa

Date	B	V	R	I	d(B)	d(V)	d(R)	d(I)	State
02.01.93	11.51				1.05				high
08.04.96	12.36	11.99	12.20	13.94	0.70	0.65	0.60	0.60	low
09.04.96	12.31	11.99	12.20	13.94	0.70	0.70	0.63	0.60	low
10.04.96	12.31	11.99	12.20	13.84	0.75	0.70	0.60	0.70	low
18.04.96	12.31	12.08	12.25	13.84	0.70	0.80	0.65	0.75	low
12.03.97	12.47	12.63	12.90	14.10	0.90	0.85	0.85	0.80	intermediate
22.04.00	11.79	11.77	11.34		0.90	0.80	0.75		high
23.04.00	11.73	11.72	11.34		1.40	1.30	1.10		high
03.05.00	12.16	12.23	12.82		0.90	0.90	0.80		intermediate
17.11.01	11.49				1.10				high
26.11.01	11.44				1.05				high

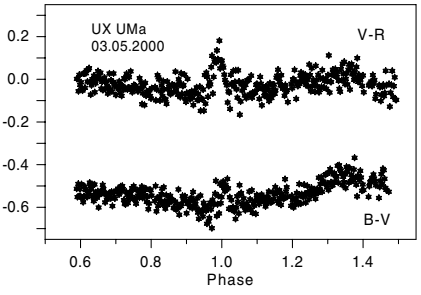

Fig. 15 Phase variations of the color indices of UX UMa

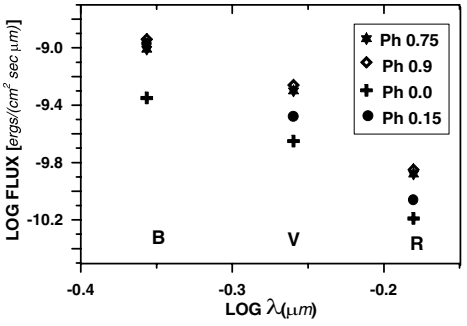

Fig. 16 Energy distributions of UX UMa at different phases

According to us the data of Dmitrienko (1994, her Fig. 3) support our assumption about the different states of UX UMa.

(11) The curves of the color indices (B-V) and (V-R) show that the star becomes bluer during the hump (Fig. 15) and redder in the middle of the eclipse (when the late star covers the primary). Although the eclipses of UX UMa lasts during the phase range 0.9–1.1 the changes of the color indices are notable only in the phases 0.95–1.05 when their values decrease. This result coincides with that of Dmitrienko (1994).

The energy distributions of the optical emission of UX UMa (Fig. 16) at phases 0.75, 0 (the middle of the eclipse), 0.9 (the phase of the maximum brightness) and 0.15 (after the eclipse) show that the fluxes in the B range are almost the same at phases 0.15, 0.75 and 0.90 while the V and R fluxes at phase 0.15 are considerably smaller than those at phases 0.75 and 0.9.

(12) The widths of the eclipses at both low and high states of UX UMa (Fig. 17) are almost equal. This means that the light increase at high state is not caused by increase of the size of the accretion disk.

(13) During our high-speed photometry the star UX UMa does not show 29-sec oscillations. This is not surprising because after their discovery (Warner and Nather, 1972) these oscillations are not always observed;

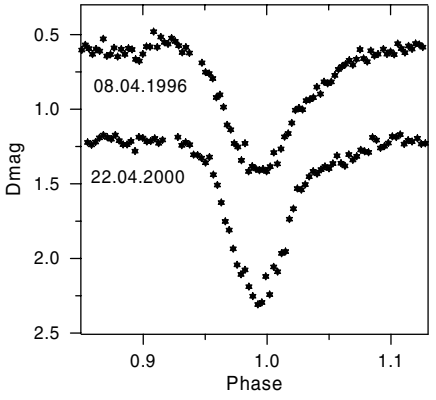

Fig. 17 The widths of the eclipses of UX UMa at high and low state

(14) Besides the flickering we found quasi-periodic oscillations on the time scale of several minutes and amplitudes below 0.01 mag (Fig. 18).

4 Analysis of the spectral data

The profile of the wide emission H_α line of UX UMa is two-peaked at the most phases. It is cut by an central absorption separating the red (R) and violet (V) emission peaks.

The H_α profile changes during the orbital cycle as well as during the different seasons. We noted the following trends of this variability:

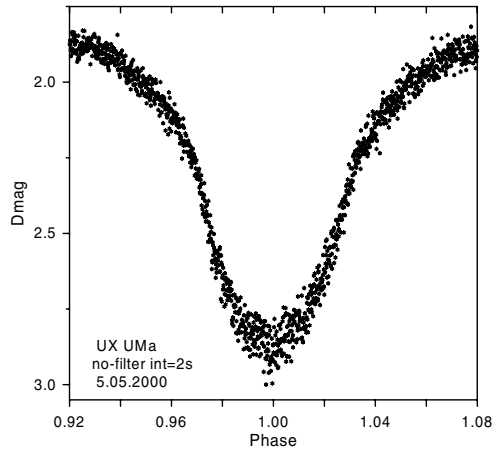

Fig. 18 Details of the eclipse of UX UMa

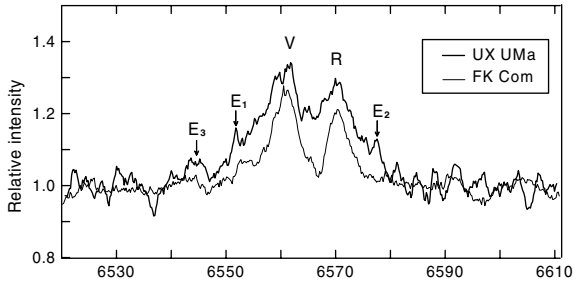

Fig. 19 The H_α line (smoothed profile) of UX UMa and FK Com at the same phase 0.75

(1) The H_α profiles have almost the same symmetric two-peaked shape at the two quadratures;
(2) The profile is one-peaked around phase 0.0 (Figs. 12 and 14) and sometimes at phases 0.3 and 0.8;
(3) There is a third emission feature between the two main peaks at some phases (Fig. 19);
(4) At the two quadratures there are pair of small almost symmetric emission features E_1 and E_2 on the outer wings of the two main peaks (Fig. 19). These features are separated by 20 Å at the first quadrature and 25 Å at the second one and have intensity around 1/2 of that of the main peaks. Moreover, at the two quadratures there is an emission feature E_3 at the blue end of the main H_α profile with width around 5 Å and intensity nearly 1/6 of that of the central peaks. The presence of these emission features on the outer wings of the two main peaks of the H_α profile may be attributed to a spiral distribution of the matter of the accretion disk;
(5) The double-peaked H_α line of the nova-like cataclysmic star UX UMa is very similar in shape to that of the disk-like star FK Com (Fig. 19) we observed by the same equipment (Kjurkchieva and Marchev, 2005).

The similarity of the H_α line of UX UMa with that of FK Com appears not only in the shape but also in:

(a) almost equal intensities of the emission peaks above the continuum level (around 0.25–0.35);
(b) almost equal widths of the absorption reversal, the two emission peaks as well as the whole H_α profile;
(c) the variable depth of the absorption reversal during the cycle;
(d) the presence of additional emission features on the main V and R peak;
(e) almost the same ratio V/R at phase 0.75.

The two-peaked H_α profile of UX UMa is typical for the emission of an accretion disk.

Although our spectral data are with low ratio S/N they allow us to obtain an approximate value of K_1 by measurement of the λ difference between the main emission peaks at the two quadratures. Adopting the value $i = 71^\circ$ (Smak, 1994a,b) we determined $K_1 = 169$ km/s. This value is near to those determined by previous authors as well as to the value of 157 km/s measured by Shafter (1984) on H_α line and used widely for UX UMa.

5 Modeling of the light curves

In order to model our data we assume the following configuration of UX UMa: the secondary is an evolved late star filling its Roche lobe (with filling $\mu = 1.0$); the spherical white dwarf with a radius R_{wd} surrounded by elliptical accretion disk. Taking into account that the flux of the white dwarf out the eclipse is constant and that the light contribution of the M2-3 V red dwarf ($T_{\rm eff} \sim 3400$ K) is small to cause the observed light fluctuations out of the eclipse, we assume that the variability of the UX UMa light curves is due to the changes of the disk flux.

We chose to model the V light curves of UX UMa corresponding to its intermediate state (from March 12, 1997 and May 3, 2000). The light curve of UX UMa from May 3, 2000 shows a dip at phase range $\varphi \sim 0.2-0.25$ that is unusual for cataclysmic variables. In contrast to the light curve from April 23, 2000 revealing an anomalous hump at phases $\varphi \sim 0.15-0.25$, the two light curves corresponding to intermediate state of the star have small humps at phases $\varphi \sim 0.8-0.9$. Obviously the hot spot model cannot fit such a type of variability with dips and humps on the light curves because the hot spot is not visible at phases $\varphi \sim 0.15-0.70$.

In order to fit the chosen light curves of UX UMa we tested two models (Fig. 20).

(a) The "hot line" model (detailed description in Khruzina, 2001) takes into account the presence of hot line near a lateral surface of the disk. We assumed that the hot line has an ellipsoidal shape with semi-axes a_v, b_v and c_v.

The contribution of the leeward side of the hot line is visible as a hump at phases $\varphi \sim 0.8-0.9$ while the

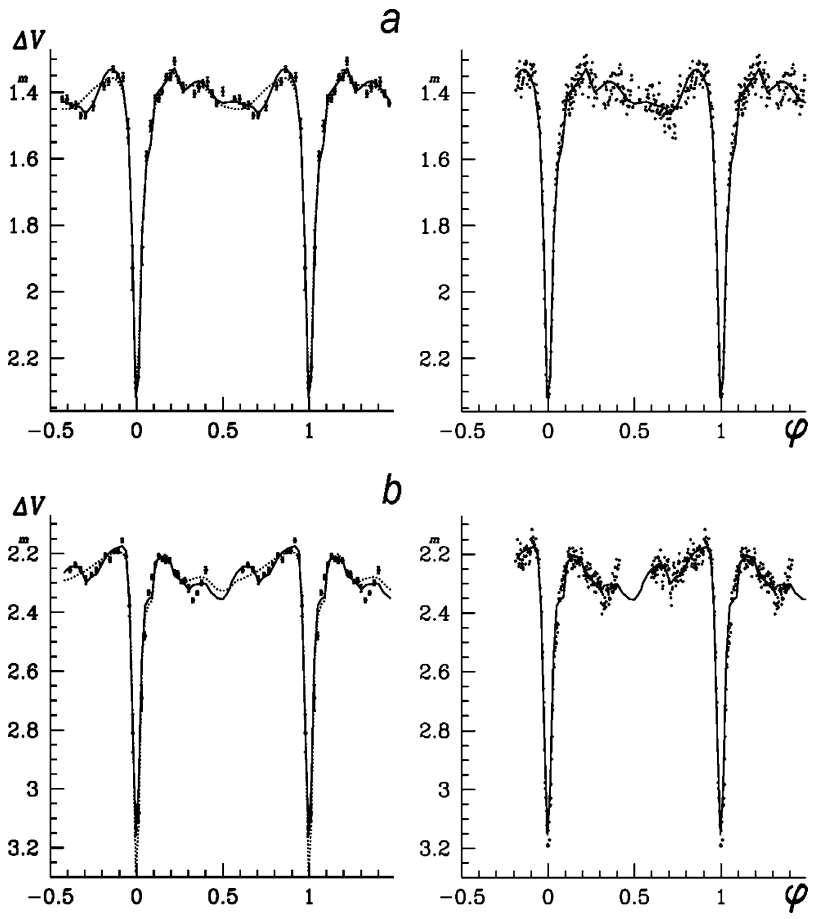

Fig. 20 On the left: the fit between the averaged V-light curves of UX UMa from March 12, 1997 (a) and May 3, 2000 (b) and the theoretical curves of the "spiral arms" model (solid lines) and "hot line" model (dash lines); On the right: the theoretical curves of the "spiral arms" model with observed nonaveraged V-light curves

contribution of the windward side of the hot line is visible as a hump at phases $\varphi \sim 0.2$ but only for the systems with an appropriate orientation of the elliptical disk and gaseous stream. If the emitting region on the hot line is very extended or the material of the hot line is outside the external disk edge (as a result of shock interaction of the gaseous stream with the inter-component envelope and disk), the contribution of the hot line appears as a hump at phases $\varphi \sim 0.4-0.6$. Under worse visibility of the hot regions of the windward side of the hot line only radiation from its leeward side may be detected which contribution appears as a hump on the light curve before the eclipse. Hence the "hot line" model is able to reproduce the irregular out-of-eclipse variations of the light curves.

(b) The "spiral arms" model takes into account contributions of the hot line as well as the spiral arms on the disk surface or at least the vertical inhomogeneities of its outer regions.

In the framework of this model we suppose that the amplitude of the logarithmic spiral wave quickly decreases to the white dwarf by the following assumptions: (a) the vertical inhomogeneity of the disk is spiral-shaped; (b) this inhomogeneity is maximum near the disk external edge and sharply decreases to the disk center; (c) the temperature into spiral arms is higher than the surrounding regions.

The correspondence of the results of such a model with the photometric data would lead to a reliable conclusion about the existence of significant thickness of the outer disk edge at the region of the spiral arm (or arms). The results of the Doppler tomography would provide an additional confirmation of the model.

We describe the distance Z of some point of a spiral arm from the middle disk plane by the expression:

$$Z = z(x, y) \cdot h \tag{2}$$

where $z(x, y)$ is the z-coordinate of the disk surface without spiral arm bulge and

$$h = \frac{\xi}{\sqrt{[\rho/R_d(\psi) - \exp(\eta(\psi - \delta - B))]^2 + \varepsilon^2}} \tag{3}$$

The parameters in the foregoing expression have the following meaning: ρ is the polar distance; ξ is the amplitude of the spiral waves; η is the angle of the logarithmic spiral; ψ is the azimuthal angle; δ is the positional angle of the spiral arm, i.e.

the angle between the disk periastrum and the radius-vector corresponding to the maximum amplitude of the spiral arm; ε is the width of the spiral arm. If the disk has two spiral arms then the position angle of the second arm is $\pi + \delta > \psi > \delta$. The last condition defines the counterclockwise direction of the spiral arms rotation and forbids the intersection of the arms each other. The values of the parameter B are different for the two spiral arms: $B = 0$ for the first arm ($\psi < \delta$) and $B = 2\pi$ for the second arm ($\psi > \pi + \delta$). Hear is expected that angular distance between crests of spiral wave arms is equal to π. In general it can differ from π.

The height of the spiral arm at the disk edge ($\rho = R_{\rm disk}$ and $\psi - B = \delta$) is

$$Z_{\rm ext} \sim z(x, y)\frac{\xi}{\epsilon}. \tag{4}$$

We assume also that the temperature of a point on the spiral arms is

$$T(x, y, Z) = T_d(x, y, z) + T_{\rm spir} \tag{5}$$

where $T_d(x, y, z)$ is the temperature of its corresponding point of the disk surface.

The two models ("hot line" and "spiral arms") require a lot of parameters for synthesis of theoretical light curves. So, our first step of the modeling procedure was to limit the ranges of the values of the searched for parameters on the basis of the results of previous analyses of spectral and photometric data of UX UMa (Table 3) in the following way: mass ratio – $q \sim 0.9-1.5$; orbital inclination – $i \sim 65-73^\circ$; radius of the white dwarf – $R_{wd} \sim 0.010-0.015a_0$; effective temperature of the white dwarf – $T_{wd} < 50000\ K$; effective temperature of the secondary – $T_{rd} \sim 3300-3500\ K$ (corresponding to M2-3 MS star); average radius of the disk – $(0.20-0.36)a_0$; disk ellipticity – $e < 0.2$.

Table 3 Parameters of UX UMa obtained from previous investigations

Parameters	1	2	3	4	5
$i,^\circ$		65	71	73	71
$M_{wd}, M_\odot$		0.5 ± 0.2	$\sim$0.45	$\sim$0.7	$\sim$0.47
$M_{rd}, M_\odot$		$\sim$0.5	$\sim$0.45	$\sim$0.48	$\sim$0.47
$q = M_{wd}/M_{rd}$		1 ± 0.4	$\sim$1	$\sim$1.45	$\sim$1
$R_{wd}, R_\odot$	0.05				0.014
$R_{rd}, R_\odot$	0.53	0.58			0.51
T_{wd}, K					52000
R_d, a_0		0.33		0.34	
$a_0, R_\odot$					1.39
z_0/R_d				$\sim$0.1	

Note. 1 – Nather and Robinson (1974); 2 – Frank et al. (1981); 3 – Bailey (1981); 4 – Smak (1994c); 5 – Baptista et al. (1995); z_0 is the semi-thickness of the outer disk; a_0 is the distance between the components.

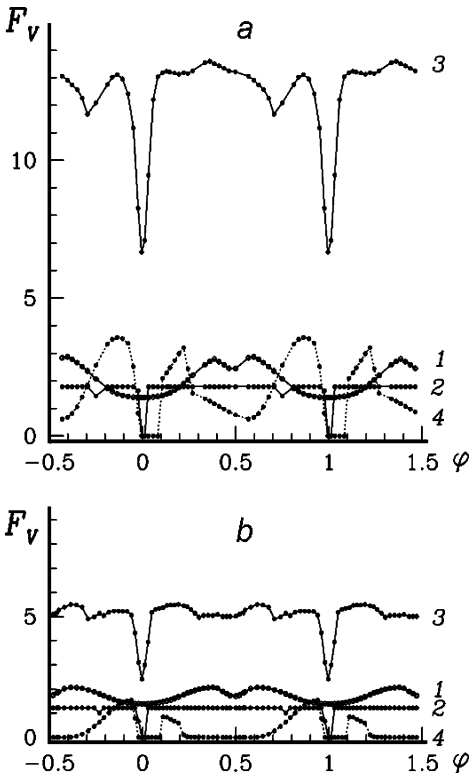

Fig. 21 Contributions of radiation from different components of the system in model "spiral structure on the disk": red (1) and white (2) dwarfs, elliptical accretion disk (3) and hot line (4) in combined flux obtained in the process of modeling V-light curves UX UMa of March 12, 1997 (a) and May 3, 2000 (b)

Other unknown parameters of both models are: (a) the temperature T_{bw} of the surface layer near the white dwarf equator; (b) the positional angles $\Delta_1 = \alpha_e - \delta$ between the top of the first spiral arm and the line connecting the components of the system and Δ_2 of second arm crest measured in counterclockwise direction; (c) the semi-axes a_v, b_v, c_v of the hot line' ellipsoid; (d) the maximum temperatures (T_1) and (T_2) at the windward side and leeward side of the hot line; (e) the semi-thickness β of the outer disk edge; (f) the parameter α_g describing the temperature distribution along the disk radius ρ according to the relation

$$T_g = T_{bw}\left(\frac{R_{wd}}{\rho}\right)^{\alpha_g} \tag{6}$$

where T_{bw} is the temperature of the inner regions of accretion disk near the white dwarf' equator. For a steady state $\alpha_g = 0.75$, i.e. every point of the disk surface radiates as a black body (α_g reaches values of $\sim$0.1 at outburst of CVs when the radiation of the accretion disk increases considerably, Djurasevic, 1996).

Table 4 Parameters of UX UMa components obtained by our modeling

	"Hot line" model		"Spiral arms" model	
Parameters	March 12, 1997	May 3, 2000	March 12, 1997	May 3, 2000
$q = M_{wd}/M_{rd}$	0.93			
i°	69.95			
White dwarf				
R_{wd}/a_0	0.0115			
T_{wd}, K	27600	27600	29830	23245
Red dwarf				
$< R_{rd}/a_0 >$	0.3971			
T_{rd}, K	3420	3415	3415	3395
Accretion disk				
e	0.172	0.188	0.168	0.158
$\alpha_e,^\circ$	140.2	145.0	87.1	81.0
a/a_0	0.327	0.322	0.358	0.332
$R_{\min}/a_0$	0.271	0.262	0.298	0.279
$R_{\max}/a_0$	0.384	0.383	0.418	0.384
$\beta,^0$	4.2	4.2	4.0	4.2
α_g	0.535	0.644	0.566	0.711
T_{bw}, K	28230	27600	30455	25655
Spiral wave in accretion disk				
ξ	–	–	0.262	0.254
T_{spir}, K	–	–	150	2447
$\Delta_1,^\circ$	–	–	77.35	79.32
$\Delta_2,^\circ$	–	–	257.35	233.2
Hot line				
a_v/a_0	0.015	0.022	0.039	0.056
b_v/a_0	0.220	0.144	0.235	0.185
c_v/a_0	0.035	0.030	0.031	0.032
T_1, K	18020	22690	23340	25195
T_2, K	3700	5995	4440	5720
χ^2	191	562	96.4	255

Remarks. α_e – longitude of the periastrum of the disk; a/a_0 – big semiaxis of the disk; $R_{\min}/a_0$, $R_{\max}/a_0$ – minimum and maximum size of the disk; a_0 – distance between the star components; χ^2 is the residual between the synthetic and observed light curves

Due to the large number of the unknown parameters we had to fix some of them at the second stage of the modeling procedure: $q = M_{wd}/M_{rd} = 0.93$; $i = 69^\circ.95$; $R_{wd} = 0.0115a_0$. The distance between mass centers of the components for $q = 0.93$, $M_{rd} = (0.45-0.48)M_\odot$ and $P_{\text{orb}} = 0.196671273$ is $a_0 = (1.36-1.39)R_\odot$. Additionally for the "spiral arms" model we fixed: $\varepsilon = 0.05$ and $\eta = 1$.

We used the method of Nelder-Meed (Himmelblau, 1972) in searching for the fitted parameters.

Table 4 presents the results of our modeling of the V-light curves of UX UMa by "hot line" and "spiral arms" models. The values of the residuals show that the second model is better for both light curves. Figure 20 shows the theoretical light curves corresponding to the parameters from Table 4. The synthetic light curves of the second model reproduce better the out-of-eclipse parts of the observational curves, especially at the phase range ($\varphi \sim 0.2-0.8$). It is due to the bigger vertical thickness of the outer disk leading to a partial covering of the hot inner disk regions as well as the white dwarf at these phases.

Figure 21 presents the contributions of the different emitting components of the system for the "spiral arms" model: red dwarf (1); white dwarf (2); accretion disk (3); hot line (4). The fluxes F_V are given in arbitrary units. They can be transformed to standard units (per unit wavelength interval) using the expression $f = 10^{-23}F_V a_0^2$ erg/s·cm^3 where a_0 is in cm.

Obviously, the out-of-eclipse fluctuations of the light curves are result mainly of the phase dependency of the contribution of the accretion disk.

In the framework of our "spiral arms" model of UX UMa we obtained that at its intermediate stage the contribution of the spiral arms to the total V flux of the disk is ∼17% and ∼30% for March 12, 1997 and May 3, 2000 respectively.

These values are slightly bigger than that obtained for the system IP Peg at outburst (Baptista et al., 2000). We explain this fact by the following reasons: IP Peg has 2 times higher mass ratio ($q \sim 1.7$); the orbital inclination of IP Peg is bigger ($i \sim 80^\circ$); the temperature of the disk of IP Peg is lower (∼3000 K, Khruzina et al., 2001).

Figure 22 shows the structure of the accretion disk of UX UMa obtained in the framework of the proposed model. It reveals the fast decreasing of the disk thickness inside spiral arms to the disk center. The good coincidence of the results of

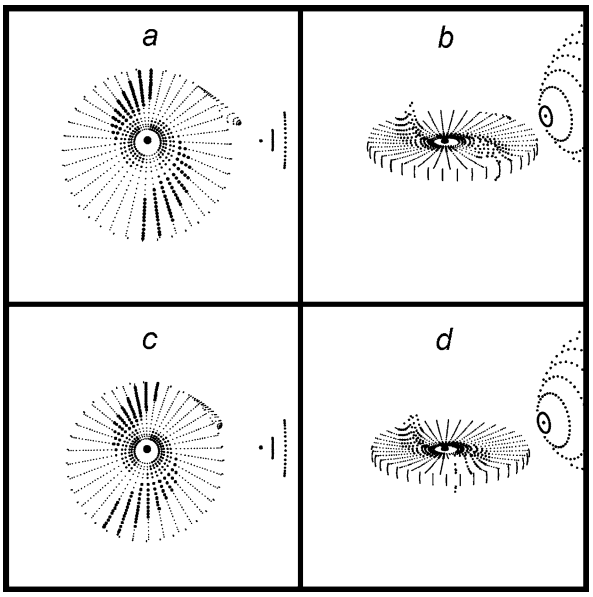

Fig. 22 The configurations of the accretion disk for $i = 0^\circ$ (a, c) and $i = 69^\circ.95$ (b, d), derived by modeling of the V light curves of UX UMa from March 12, 1997 (a, b) and May 3, 2000 (c, d) (the thick points shown the spiral arms)

our model and the observational light curves of UX UMa is a strong argument for the increasing vertical thickness of the outer disk regions (dense structures) covering the emission of its internal regions and (sometimes) the white dwarf at phases ∼0.7 and ∼0.2 (see Fig. 21). The orbital phase of the dip on the light curve depends on: (a) the positional angle of the dense structures at the disk edge; (b) the form of the dense structures; (c) their temperature; (d) the size and orientation of the disk; (e) the orbital inclination.

We obtained for UX UMa that the positional angle of the first arm is $\sim 77^\circ.4$ for March 12, 1997 and $\sim 79^\circ.3$ for May 3, 2000 (Fig. 22). Crests of second arms of the spiral wave are displaced accordingly on 180° and 154° toward counterclockwise relative the line connecting the components of the system. This configuration is similar to those determined for other cataclysmic variables (Baptista et al., 2000). So far there is not a reasonable explanation for the different orientation of the spiral arms (or denser structures at outer disk) during the different seasons.

6 Conclusion

The main results of our investigation on UX UMa are:

(1) The out-of-eclipse brightness of the system and the depth of the eclipse changes in different time scales while the width of the eclipse remains constant;
(2) The wide two-peaked emission H_α line of UX UMa at the most phases is typical for the emission of an accretion disk;
(3) We attributed the observed features of the light curves as well as the features of the H_α profile of UX UMa to an inhomogeneity of the accretion disk;
(4) We proposed "spiral arm" model for a fitting of the irregularities of the UX UMa light curves at intermediate state. It reproduces well the observational data. As a result we obtained a disk with two spiral arms. The azimuthal extent of the spiral arms is ∼90° and their light contribution is about 17–30% of the total V flux of the disk. The orientation of these spiral arms is different during different seasons;
(5) The obtained two dense structures at the outer disk covering partially the inner hot disk and the white dwarf at orbital phases ∼0.7 and ∼0.2 is in agreement with the predictions of the theoretical computations (Bisicalo et al., 2005). Such a disk structure would be confirmed by Doppler tomography of spectral data.

Acknowledgements The research was supported partly by funds of project F1411/2004 of the Bulgarian Ministry of Education and Science as well as project No. 4/2006 of Shumen University, by the Russian Foundation for Basic Research (project no. 05-02-17489, 06-02-16411), the program "Leading Scientific Schools of Russia" (grant no. NSh-388.2003.2), the program "Russian Universities Fundamental Studies" (project no. UR.02.03.012/1), the project no. 146003 of the Ministry of Science and Environmental Protection of Serrbia.

References

Bailey, J.: MNRAS **197**, 31 (1981)
Baptista, R. et al.: ApJ **448**, 395 (1995)
Baptista, R., Harlaftis, E.T., Steeghs, D.: MNRAS **314**, 727 (2000)
Bisikalo, D., Boyarchuk, A., Kuznetsov, O., Chechetkin, V.: Astron. Rep. **41**, 786 (1997a)
Bisikalo, D., Boyarchuk, A., Kuznetsov, O., Chechetkin, V.: Astron. Rep. **41**, 794 (1997b)
Bisikalo, D., Boyarchuk, A., Chechetkin, V. et al.: MNRAS **300**, 39 (1998)
Bisikalo, D., Kaigorodov, P., Boyarchuk, A., Kuznetsov, O.: Astron. Rep. **49**, 701 (2005)
Bisikalo, D., Kaigorodov, P., Boyarchuk, A., Kuznetsov, O.: ApSS. (tmp) **22** (2006)
Borkowski, G.: Internal report of Astron. Inst. in Torun, Poland (1988)
Bruch, A.: A&A **359**, 998 (2000)
Djurasevic, G.: ApSS **240**, 317 (1996)
Dmitrienko, E.: Izv. Kr. Ap. Obs. **83**, 131 (1991)
Dmitrienko, E.: Izv. Kr. Ap. Obs. **86**, 62 (1992)
Dmitrienko, E.: Astr. Let. **20**, 104 (1994)
Frank, J., King, A., Sherrington, M. et al.: MNRAS **195**, 505 (1981)
Harlaftis, E., Marsh, T.: A&A **308**, 97 (1996)
Himmelblau, D.: Applied Nonlinear Programming, McGraw-Hill, New York, p. 163 (1972)
Holm, A., Panek, R., Schiffer, F.: ApJ **252**, L35 (1982)
Johnson, H., Perkins, B., Hiltner, W.: ApJSS **1**, 91 (1954)
Khruzina, T.: Astron. Rep. **45**, 255 (2001)
Khruzina, T.: Astron. Rep. **49**, 783 (2005)
Khruzina, T., Cherepashchuk, A., Bisikalo, D. et al.: Astron. Rep. **45**, 538 (2001)

Khruzina, T., Cherepashchuk, A., Bisikalo, D. et al.: Astron. Rep. **47**, 621 (2003a)
Khruzina, T., Cherepashchuk, A., Bisikalo, D. et al.: Astron. Rep. **47**, 214 (2003b)
Kjurkchieva, D., Marchev, D.: A&A **434**, 221 (2005)
Knigge, C., Drake, N., Long, K. et al.: ApJ **499**, 429 (1998)
Kreiner, J., Krzesinski, J., Pokrzywka, B. et al.: in Elliot, I., Buttler, C. (eds.), IAU Coll. No 136, poster papers on stellar photometry. Dublin Institute for Advanced Studies, p. 80 (1993)
Kreiner, J., Kim, C., Nha Il-Seong: An atlas of O-C diagrams of eclipsing binary stars. Krakow Pedagogical University Press (2001)
Krzeminski, W., Walker, M.: ApJ **138**, 146 (1963)
Krzesinski, J., Wojcik, K.: A&A **280**, 338 (1993)
Kuznetsov, O., Bisikalo, D., Boyarchuk, A. et al.: Astron. Rep. **45**, 872 (2001)
Linnell, A.: Sky & Telescope **8**, 166 (1949)
Makita, M., Miyawaki, K., Matsuda, T.: MNRAS **316**, 906 (2000)
Mandel, O.: Var. Stars **15**, 480 (1965)
Meyer, F., Meyer-Hoffmeister, E.: A&A **121**, 29 (1983)
Naylor, T., Koch-Miramond, L., Ringwald, F., Evans, A.: MNRAS **282**, 873 (1996)
Nather, E., Robinson, E.: ApJ **190**, 637 (1974)
Schlegel, E., Honeycutt, R., Kaitchuck, R.: ApJS **53**, 397 (1983)
Shafter, A.: AJ **89**, 1555 (1984)
Smak, J.: AcA **20**, 312 (1970)
Smak, J.: AcA **44**, 59 (1994a)
Smak, J.: AcA **44**, 257 (1994b)
Smak, J.: AcA **44**, 265 (1994c)
Smirnov, O.: in ASP Conf. Ser. Vol. 26, Astronomical Data Analysis Software and Systems 1, p. 344 (1992)
Steeghs, D.: in Boffin, H.M.J., Steeghs, D., Cuypers, J. (eds.), Astrotomography, Indirect imaging methods in observational astronomy. Lecture Notes in Physics, Vol. 573, p. 45 (2001)
Suleimanov, V., Neustroev, V., Borisov, N., Fioktistova, I.: RevMexAA **20**, 270 (2004)
Walker, M., Herbig, G.: ApJ **120**, 278 (1954)
Warner, B., Nather, R.: MNRAS **159**, 429 (1972)
Wood, J., Naylor, T., March, T.: MNRAS **274**, 31 (1995)